Stratification of acute myocardial and endothelial cell injury, salvage index and final infarct size by systematic microRNA profiling in acute ST-elevation myocardial infarction

Sam Dawkins[a], Janet E. Digby[a], T. Grant Belgard[b], Regent Lee[a], Giovanni Luigi De Maria[c], Adrian P. Banning[c], Rajesh K. Kharbanda[a,c], Oxford Acute Myocardial Infarction (OxAMI) Study, Manuel Mayr[d], Robin P. Choudhury[a,c] and Keith M. Channon[a,c]

Aim **Acute injury and subsequent remodelling responses to ST-segment elevation myocardial infarction (STEMI) are major determinants of clinical outcome. Current imaging and plasma biomarkers provide delayed readouts of myocardial injury and recovery. Here, we sought to systematically characterize all microRNAs (miRs) released during the acute phase of STEMI and relate miR release to magnetic resonance imaging (MRI) findings to predict acute and late responses to STEMI, from a single early blood sample.**

Methods and results **miRs were quantified in blood samples obtained from patients after primary PCI (PPCI) for STEMI. Cardiac MRI (cMRI) was performed to quantify myocardial edema, infarct size and salvage index. Regression models were constructed to predict these outcomes measures, which were then tested with a validation cohort. Transcoronary miR release was quantified from paired measurements of coronary artery and coronary sinus samples. A cell culture model was used to identify endothelial cell–derived miRs.**

A total of 72 patients undergoing PPCI for acute STEMI underwent miR analysis and cMRI. About >200 miRs were detectable in plasma after STEMI, from which 128 miRs were selected for quantification in all patients. Known myocardial miRs demonstrated a linear correlation with troponin release, and these increased across the transcoronary gradient. We identified novel miRs associated with microvascular injury and myocardial salvage. Regression models were constructed using a training cohort, then tested in a validation cohort, and predicted myocardial oedema, infarct size and salvage index.

Conclusion **Analysis of miR release after STEMI identifies biomarkers that predict both acute and late outcomes after STEMI. A novel miR-based biomarker score enables the estimation of area at risk, late infarct size and salvage index from a single blood sample 6 hours after PPCI, providing a simple and rapid alternative to serial cMRI characterization of STEMI outcome.** ***Coron Artery Dis*** **35: 122–134**

Coronary Artery Disease 2024, **35**:122–134

Keywords: ischemia, microcirculation, MiR, myocardial infarction, STEMI

[a]Division of Cardiovascular Medicine, British Heart Foundation Centre of Research Excellence, Radcliffe Department of Medicine, University of Oxford, John Radcliffe Hospital, Oxford, UK, [b]The Bioinformatics CRO, Niceville, Florida, USA, [c]Oxford Heart Centre, National Institute for Health (NIHR) Oxford Biomedical Research Centre, Oxford University Hospitals NHS Foundation Trust, Oxford and [d]King's British Heart Foundation Centre, King's College London, London, UK

Correspondence to Professor Keith M. Channon, Division of Cardiovascular Medicine, Radcliffe Department of Medicine, University of Oxford, John Radcliffe Hospital, Oxford, OX3 9DU, UK
Tel: +44 (0) 1865 234657; fax: +44 (0) 1865 234658; e-mail: keith.channon@cardiov.ox.ac.uk

Received 21 May 2023 **Accepted** 12 August 2023.

Introduction

Acute ST-elevation myocardial infarction (STEMI) remains a major cause of death and the leading cause of chronic heart failure [1]. Primary percutaneous coronary intervention (primary PCI) has transformed the early treatment of myocardial infarction, reducing mortality and morbidity by rapidly re-opening the occluded coronary artery, with major efforts in healthcare policy and guidelines aimed at minimizing delays in patient pathways and 'door to balloon' times [2,3]. However, prompt restoration of vessel patency does not necessarily lead to effective myocardial reperfusion. Indeed, apparently, similar patients with good angiographic primary PCI results may have very different outcomes in terms of myocardial salvage and infarct size [4]. These differences are driven by unpredictable heterogeneity in ischemia-reperfusion injury, coronary microvascular dysfunction, inflammation and myocardial remodeling [5,6].

Serial measurements of plasma troponin can quantify myocardial injury after STEMI, and also predict the subsequent risk of left ventricular impairment and 1-year

Supplemental Digital Content is available for this article. Direct URL citations appear in the printed text and are provided in the HTML and PDF versions of this article on the journal's website, www.coronary-artery.com.

DOI: 10.1097/MCA.0000000000001284

mortality [7]. Cardiac MRI (cMRI) can quantify the 'area at risk' early after STEMI, and the final infarct size on a second scan weeks or months after STEMI, enabling estimation of the 'salvage index' [8]. However, these approaches to patient stratification after STEMI rely on techniques that quantify the biochemical and mechanical consequences of acute myocardial injury and subsequent myocardial necrosis in the days, weeks and months after STEMI. There are no current clinically applicable biomarker approaches that incorporate other critical biological components of the local and systemic response to STEMI, such as microvascular injury and inflammation. A more comprehensive biologically-driven biomarker strategy for patient stratification could identify those who require more intensive or targeted therapies, vs. those who could be discharged earlier for expedited recovery [9]. Furthermore, a biomarker profile with integrated biological readouts related to multiple components of the acute response to STEMI, at a single early time point, could potentially obviate the need for repeated imaging to quantify early and late outcomes of STEMI.

MicroRNAs (miRs) are small non-coding RNAs that are detectable in plasma when released from tissues or cells [10]. Plasma miRs are stable during processing and storage, making them potentially useful biomarkers [11]. Several previous studies have shown that a number of miRs, known as 'myomiRs', are released from the myocardium and are detectable in plasma after acute myocardial infarction [12]. Some myomiRs may have utility as biomarkers for the early diagnosis of myocardial infarction, and selected miRs have also been shown to correlate with important clinical outcomes such as infarct size [13,14]. However, these known myomiRs relate to myocardial necrosis, which is already highly quantifiable by measuring serum troponin levels, so are of uncertain additional utility in improving patient stratification after STEMI. In contrast, an unbiased and systematic evaluation of miR release after STEMI could provide important new insight into the wider pathophysiologic mechanisms of myocardial injury and remodeling, including microvascular injury, platelet activation, inflammation, myocardial injury and salvage. These findings would have implications for patient stratification, and for targeting and evaluating novel therapeutic approaches.

Accordingly, we sought to systematically quantify all detectable human miRs in plasma immediately after STEMI in patients undergoing PPCI. First, we identified miRs correlating with clinical parameters such as troponin release, infarct size and acute myocardial edema. Additionally, we carried out detailed miR analysis on paired coronary artery and coronary sinus plasma samples to identify miRs released down the coronary gradient. In an in vitro experiment, we quantified miR release from human umbilical vascular endothelial cells (HUVECs) and compared these findings with those from human plasma samples. We then used principal component analysis (PCA) to provide a statistically robust, unbiased identification of potential biomarker miRs in acute STEMI. From these miR profiles, we built multiple linear regression models to predict the important clinical outcomes following STEMI, including acute myocardial edema, infarct size and salvage index. Validating these observations in a second cohort of patients established a predictive biomarker strategy for patient stratification after STEMI, based on a single venous blood sample obtained early after PPCI.

Methods

Study patients

Patients undergoing emergency PPCI for STEMI were recruited as part of the Oxford Acute Myocardial Infarction (OxAMI) study. Diagnosis of STEMI was established on the basis of chest pain, ST-segment elevation of 0.2 mV in at least 2 contiguous leads on ECG and thrombolysis in myocardial infarction (TIMI) grade 0 flow on initial angiography. Verbal assent for participation was obtained at the time of PPCI [15]. Informed written consent for continued participation was obtained within the following 24 h. The study protocol and consent process were approved by the local Research Ethics Committee (REC number 11/SC/0397).

Angiography and PCI

Patients with STEMI received aspirin (300 mg) and clopidogrel (600 mg) or ticagrelor (180 mg) loading before PPCI and were treated with intravenous bivalirudin and/or heparin during the procedure. The coronary intervention was performed via the radial artery. Epicardial coronary reperfusion was established using a thrombus aspiration catheter and/or balloon pre-dilatation. The culprit lesion was treated with drug-eluting stent deployment, and dual antiplatelet therapy with aspirin and clopidogrel or ticagrelor for 12 months. During primary PCI, coronary artery, coronary sinus and peripheral venous blood samples (serum and plasma) were obtained. Further peripheral venous blood samples were obtained 6, 24 and 48 h after the procedure.

Blood processing

Plasma samples were immediately centrifuged and the upper plasma layer was transferred to a new test tube and centrifuged a second time to obtain platelet-poor plasma, confirmed by platelet count. Serum samples were centrifuged once. Platelet-poor plasma and serum were divided into aliquots and placed into storage at –80 °C [16].

Clinical parameters

Aliquots of serum collected at 0, 6, 24 and 48 h were used for troponin-I analysis. These samples were processed in batches by the local clinical biochemistry laboratory using an immunoassay technique on a Siemens Centaur XP analyzer. The four troponin measurements were used

to calculate an area under the curve (AUC) measurement using the trapezoid rule (GraphPad Prism version 8, La Jolla, CA, USA).

Electrocardiograms were acquired on arrival at the cath lab and 30 min after the procedure. ST-elevation in the worst affected lead was measured using ImageJ (National Institutes for Health, Bethesda, MA, USA) and used to calculate the percentage ST-segment resolution.

Cardiac MRI quantification of area at risk and infarct size

STEMI patients underwent a cardiac magnetic resonance scan (MRI) within 48 h of admission and 6 months later. Left ventricular function and myocardial injury were assessed in matching short-axis slices using Steady State Free Precession, T2-weighted and late gadolinium enhancement (LGE) imaging after the administration of 0.1 mmol/kg contrast agent [*Doltarem (gadoterate meglumine), Guerbet Groupe, Paris, France*], as previously described [17,18].

Assessing the effect of hypoxia on endothelial cells

Using hypoxic chambers (Invivo$_2$ 400 Hypoxia Workstation, Baker Ruskinn), HUVECs (PromoCell GmbH, Heidelberg, Germany) in cell culture medium were exposed to hypoxia (control group 21% oxygen, hypoxia group 1% oxygen) for 24 h. The cell supernatant was then centrifuged, and snap-frozen to allow subsequent miR analysis. The effect of hypoxia on cell viability was assessed using an MTT (3-(4,5-dimethylthiazol-2-yl)-2,5-diphenyltetrazolium bromide) luminescent cell viability assay (CellTiter Glo; Promega, Madison, WI, USA).

MicroRNA extraction and quantification by real-time PCR

Circulating microRNAs were isolated from plasma using the miRCURY RNA Isolation Kit for Biofluids (Exiqon, Vedbaek, Denmark) according to the manufacturer's instructions. Bacteriophage MS2 (Roche, Basel, Switzerland) was added as a carrier RNA to improve reproducibility and yield. Reverse transcription was carried out using the miRCURY universal cDNA synthesis kit II (*Exiqon*). cDNA was diluted to a 1:50 concentration. Quantitative real-time PCR was carried out with the QuantStudio 12K Flex Real-Time PCR system (ThermoFisher Scientific, Waltham, MA, USA) using custom-designed 384 well plates.

Spike-in controls were added at each stage of the process to confirm sample quality and technical success. Positive controls, miRs for detection of sample hemolysis in addition to synthetic spike-in RNA in different (1/10/100 fold) concentrations to confirm efficient RNA isolation. Quality control criteria were pre-specified: positive controls must be detected, hemolysis should be absent and all three RNA spike-in controls should be detected. If these criteria were met, a sample was determined to be of sufficient quality to be included in the analysis. If not, a further aliquot of the sample was processed and if the sample still failed to meet the quality control criteria, it was excluded.

In an initial 'discovery' experiment, an unbiased qPCR panel of 768 miRs including controls was used to profile the time course of all miRs released after STEMI (0, 6, 24 and 48 h after primary PCI). We used these results to select the optimum time-point and to design a custom PCR plate of 384 miRs with controls, that was used to analyze miR release. Finally, we designed a custom panel to detect 128 miRs with controls to analyze samples from the larger 'validation' cohort of patients. The criteria for inclusion in the final set of 128 miRs were as follows: stable reference miRs for normalization, any miRs reported to be differentially expressed in myocardial infarction identified by literature search and the most strongly correlated miRs with one of multiple clinical parameters [e.g. troponin release, infarct size, microvascular obstruction (MVO), myocardial edema] (see Supplementary data figure 1, Supplemental digital content 1, *http://links.lww.com/MCA/A599* for plate design). The 128 miR custom panel was used for miR analysis of the PPCI coronary artery and coronary sinus samples, with the same reference miRs used for normalization.

MicroRNA pre-processing and analysis

Normalization was carried out using stable reference miRs identified using the Normfinder algorithm, as previously described [19]. To allow PCA, missing data were imputed using K-nearest neighbor (KNN) imputation as previously described [20]. Relationships between known myomiRs and troponin release were established using simple correlation. miRs correlating with other outcome measures, such as infarct size and myocardial edema, were identified.

Principal component analysis

PCA was carried out to identify which miRs explained the most variance in the dataset. Correlations between each miR and clinical readouts of early and late myocardial injury were then shown in a heatmap, with miRs sorted by principal component.

Model development

Multiple regression models were developed to predict infarct size, myocardial edema and salvage index. Patients were randomly grouped into training (80%) and validation (20%) cohorts. Prior to randomization patients were binned by infarct size to ensure distribution of infarct sizes across both groups. Using the training cohort, we used automatic linear modeling [21] (SPSS version 24.0, IBM Corporation, Armonk, NY, USA) to identify miRs to use in regression models to predict infarct size, myocardial

Table 1 Patient characteristics

	All patients N = 72		Training cohort N = 53		Validation cohort N = 19		*P* value
General characteristics							
Age (mean, range)	63.8	(42–90)	64.8	(42–90)	64.8	(50–87)	0.71
Male	58	80.6%	42	79.2%	16	84.2%	0.64
Creatinine (median, range) (μmol/L)	73	(37–135)	73	(37–135)	75	(51–90)	0.50
Culprit vessel							0.63
Left anterior descending	36	50.0%	25	47.2%	11	57.9%	
Circumflex	7	9.7%	6	11.3%	1	5.3%	
Right coronary artery	29	40.3%	22	41.5%	7	36.8%	
Comorbidities							
Diabetes mellitus							0.15
Oral medication	3	4.2%	3	5.7%	0	0%	
Insulin	1	1.4%	0	0%	1	5.3%	
Chronic kidney disease	0	0%	0	0%	0	0%	NA
Smoking							0.16
Current	21	29.2%	18	34.0%	3	15.8%	
Ex	25	34.7%	19	35.8%	6	31.6%	
Lung disease	8	11.1%	4	7.5%	4	21.1%	0.20
Coronary artery disease	16	22.2%	13	24.5%	3	15.8%	0.53
Previous MI	2	2.8%	1	1.9%	1	5.3%	0.46
Previous PCI	0	0%	0	0%	0	0%	NA
Previous CABG	0	0%	0	0%	0	0%	NA
Hypercholesterolemia	22	30.6%	16	30.2%	6	31.6%	0.91
Hypertension	24	33.3%	17	32.1%	7	36.8%	0.71
Peripheral vascular disease	0	0%	0	0%	0	0%	NA
Cerebrovascular disease	1	1.4%	0	0%	1	5.3%	0.09
Valvular heart disease	0	0%	0	0%	0	0%	NA
Heart failure	0	0%	0	0%	0	0%	NA
Early outcome							
Troponin, peak (μg/L)	83.75	2.48–929.5	90.14	2.48–922	51	7.58–929.5	0.62
Troponin, AUC 0-48 h (μg/L)	2400.5	56.61–17,201	2462	56.61–17,201	1774	272.8–12 697	0.47
Myocardial edema (g)	34.2	5.8–84.8	37.7	5.8–72.0	27.6	13–84.8	0.66
Microvascular obstruction (g)	0.4	0–12.3	0.4	0–12.3	0.3	0–11.8	0.41
ST-elevation post-PCI (mm)	1.3	0–6.0	1.6	0–6.0	1.3	0–3.4	0.56
ST resolution (%)	64.2%	-22–100%	64.2%	-22–100%	58.9%	5.7–100%	0.85
Late outcome							
Infarct size (g)	10	1–38	11	1–37	10	1–38	0.68
Ejection fraction (%)	55	20–84	57	20–84	48	37–61	0.07
Salvage index (%)	65%	21–93%	65%	21–94%	64%	37–90%	0.50

The table shows the clinical details of patients with STEMI. Chronic kidney disease was defined as baseline creatinine value over 200 μmol/L. Drugs on admission refer to medications taken regularly pre-admission and does not include loading doses of aspirin and ticagrelor/clopidogrel prior to PCI. To determine whether there was a difference between training and validation cohorts, a chi-squared test was performed for discrete variables and an unpaired t-test for continuous variables.

edema and salvage index. These models were then used to predict actual values for the training and validation cohorts. Correlations between actual and predicted values were then calculated to assess the accuracy of the models.

Statistical analysis

Raw data were imported into Genex (MultiD, Göteborg, Sweden) for pre-processing and normalization. These data were then exported to SPSS for binning by infarct size, randomization into training and validation cohorts and further statistical analysis. Prism version 8 (GraphPad) was used for graph drawing, to calculate troponin AUC (using the trapezoid rule) and to draw heatmaps. Any clinical variables that were not normally distributed were log-transformed before analysis. KNN Imputation was carried out using R (R Foundation for Statistical Computing, Vienna, Austria).

Results

Patient population

Seventy-two patients undergoing PPCI for STEMI were recruited with a median age of 64 years (range 42–90) of whom 58 (80.6%) were male. Clinical characteristics are shown in Table 1. The culprit vessel was the left anterior descending artery in 36 (50%), the circumflex artery in 7 patients (9.7%) and the right coronary artery in 29 (40%). The median time between chest pain onset and start of procedure was 123 min (range 42–1289 min). Median door to balloon time was 28 min (range 7–50).

Systematic detection and quantification of miRs after STEMI

RNA isolation and reverse transcription was carried out in plasma samples collected at 0, 6, 24 and 48 h after PPCI. First, a discovery experiment using samples from six patients was carried out using an unbiased panel of 768 miRs and controls. Over 200 miRs were detected at each time point (mean number of miRs detected with cycle threshold (CT) value ≤37 at 0 h: 211; 6 h: 240; 24 h: 227; 48 h: 248) and miR concentration was consistent across all time points (mean CT value at 0 h: 32.9; 6 h: 32.0; 24 h: 32.8; 48 h: 32.3) (Supplementary data figure 2, Supplemental digital content 1, *http://links.lww.com/MCA/A599*).

More samples met all pre-specified quality control criteria at 6 hours than at the other time points (67% at 0 h; 100% at 6 hours; 83% at 24 and 48 h) (Supplementary

Fig. 1

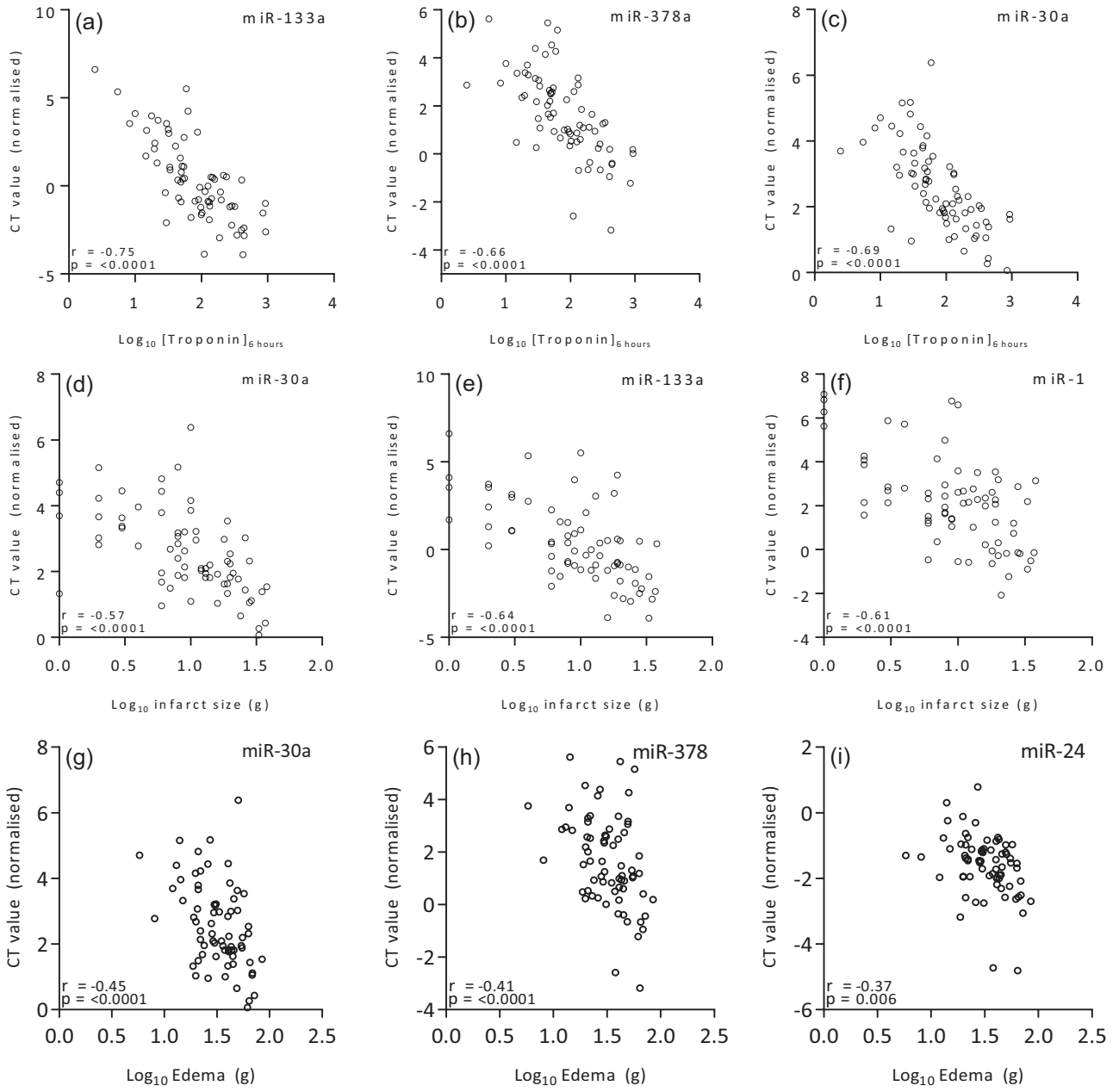

MicroRNA correlation with clinical parameters. (a–c) The relationship between selected miRs and troponin release. Each panel shows the relationship between a different miR and troponin AUC 0–48 h. (d–f) The relationships between selected miRs and infarct size measured by CMR at 6 months. Each panel shows the relationship between a different miR and infarct size. (g–i) The relationships between selected miRs and myocardial edema (area at-risk) measured my CMR within 48 h. Each panel shows the relationship between a different miR and myocardial edema. Troponin AUC, infarct size and myocardial edema are not normally distributed and were therefore $\log_{10}$ transformed. All CT values were normalized to six reference miRs. Spearman correlation was calculated for each miR and the relevant clinical parameter. Correlation coefficient (r) and significance (p) are shown in the boxes. All miRs were normalized to the six most stable miRs (identified using the Normfinder algorithm [18]). Troponin AUC, area under the curve of four troponin measurements taken at 0/6/24/48 h (μg/L) calculated using the trapezoid rule. CT, cycle threshold.

data figure 3, Supplemental digital content 1, *http://links.lww.com/MCA/A599*). The 6-hour time point was therefore selected for further miR analysis. In samples from 14 patients, the 768 miRs and controls were triaged to a 384 miR panel, by excluding miRs detected in fewer than two samples. In samples from the remaining 52 patients, a 128 miR panel was selected on the basis of the strongest correlations with clinical parameters, or previously reported relationships with myocardial injury.

To validate the sample collection and analysis methods, we first demonstrated the relationship between a

Fig. 2

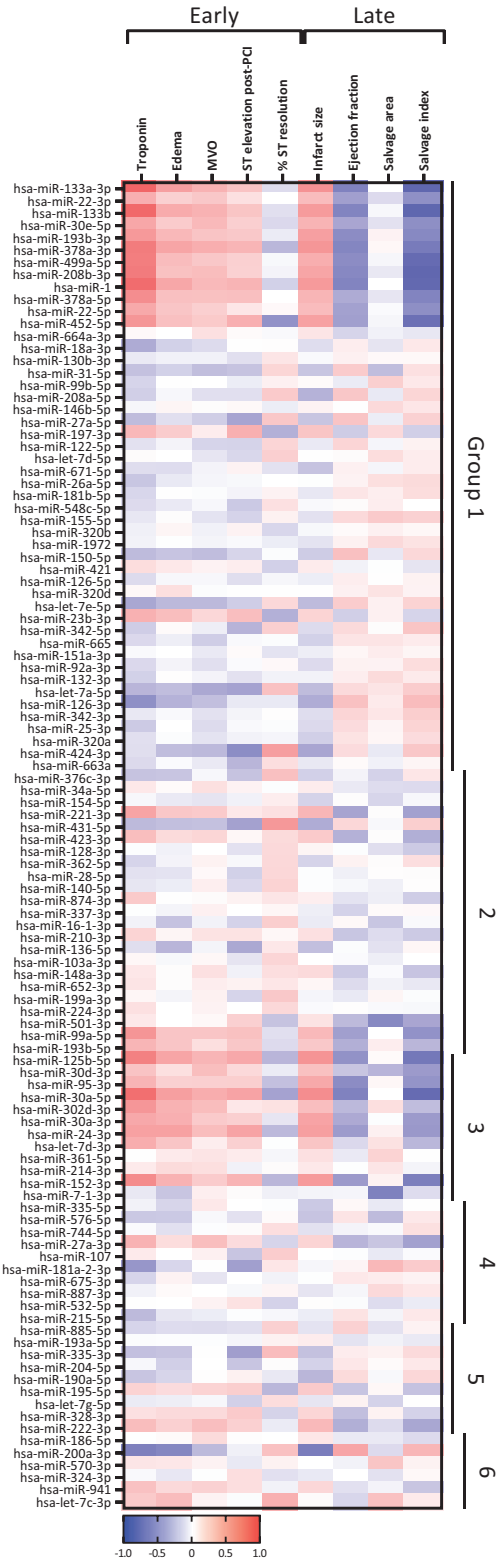

Heatmap demonstrating the relationship between miR release and clinical parameters. A Pearson correlation between each miR (normalized CT value) and each clinical parameter was calculated. Principal component analysis was carried out to identify miRs which groups of miRs were statistically related. In this heatmap, miRs are sorted according to the strength of their correlation with their dominant principal component. Troponin, troponin area under the curve using four measurements between 0 and 48 h; Edema, myocardial edema measured by cardiac MRI within 48 h; MVO, microvascular obstruction measured by cardiac MRI within 48 h (binary variable); ST-elevation post-PCI, residual ST-elevation within 30 min of primary PCI (mm); % ST resolution, ST-segment resolution between pre- and 30 min post-PCI ECGs (%). Group numbers refer to principal components. Raw correlation coefficient data are shown in Supplementary data figure 5, Supplemental digital content 1, *http://links.lww.com/MCA/A599*.

known myocardial miR (miR-133a [22]) and troponin at 6 hours (Fig. 1a), and we identified additional miRs showing a strong correlation with troponin (Fig. 1b and c). We then identified miRs showing a strong correlation with infarct size quantified by late gadolinium enhancement on cMRI at 6 months (Fig. 1d–f) and area at risk quantified by the area of acute myocardial edema on T2W imaging in the first 48 h after STEMI (Fig. 1g–i).

Next, we constructed a heatmap to gain a broader understanding of the relationship between miR release and key indicators of early and late myocardial injury. To identify groups of related miRs, PCA was carried out and miRs were then shown in the heatmap sorted according to the strength of their correlation (whether positive or negative) with their dominant principal component (Fig. 2).

We tested for associations between miRs and markers of early myocardial injury such as troponin AUC, acute myocardial edema and presence of MVO measured by CMR at 24 h, residual ST-segment elevation and ST-segment resolution after PPCI. We also tested for associations between miRs and markers of late outcome, such as infarct size, LV ejection fraction, salvage area and salvage index, determined by cMRI 6 months after STEMI.

We found that 30 principal components accounted for 90% of the variance in the dataset (Supplementary data figure 4, Supplemental digital content 1, *http://links.lww.com/MCA/A599*). There were striking patterns of association between individual miRs within each principal component and both early and late outcome measures after STEMI (Figure 2, Supplementary Data Figure 4, Supplemental digital content 1, *http://links.lww.com/MCA/A599*). In principal component 1, there were strong positive correlations between known myomiRs and markers of acute myocardial injury and negative associations with indicators of late LV function and myocardial salvage. However, we also identified additional miRs not previously identified as myomiRs, including miRs-30a-5p, 125b-5p, 152-3p, 378a-3p and 452-5p. miRs in principal component 3 were also strongly associated with myocardial injury, including miRs-125b-5p and 30a-5p.

Table 2 MicroRNAs used for regression models or showing a strong correlation with clinical parameters

			Model			MicroRNA correlation			
MicroRNA	Tissue origin[35]	Putative roles	Infarct size	Edema	Salvage	Troponin	Edema	Infarct size	Salvage
hsa-miR-7-1-3p	Nervous system	Tumor suppressor[36]							
hsa-miR-18a-3p	Spleen	Tumor suppressor[37]							
hsa-miR-23b-3p	Ubiquitous	Tumor suppressor[38]							
hsa-miR-99a-5p	Ubiquitous	Tumor suppressor[39]							
hsa-miR-145-3p	Digestive tract	Tumor suppressor[40]							
hsa-miR-151a-3p	Ubiquitous	Repression of breast cancer metastasis[40]							
hsa-miR-154-5p	Nervous system	Tumor promoter[41]							
hsa-miR-200a-3p	Endocrine Renal[28]	Repression of breast cancer metastasis[30]							
hsa-miR-219a-5p	Nervous system	Tumor suppressor[42]							
hsa-miR-299-5p	Nervous system	Regulates apoptosis[41]							
hsa-miR-362-5p	Muscle, skin	Tumor promoter[43]							
hsa-miR-381-3p	Nervous system	Tumor suppressor[44]							
hsa-miR-423-3p	Ubiquitous	Known myocardial miR, marker of left ventricular remodelling[45]							
hsa-miR-424-3p	Nervous system, lung	Tumor suppressor[46]							
hsa-miR-501-3p	Nervous system	Tumor promoter[47]							
hsa-miR-887-3p	Solid organs, gut	Tumor promoter[48]							
hsa-miR-941	Nervous system	Tumor suppressor[49]							
hsa-let-7a-5p	Nervous system	Inflammation[50]							
hsa-let-7c-3p	Nervous system	Apoptosis[51]							
hsa-let-7d-5p	Nervous system	Tumor promoter[52]							
hsa-let-7e-5p	Nervous system	Inflammation, endothelial function[53]							

All microRNAs used in the predictive models for edema, infarct size and myocardial salvage, with their tissue origins and putative roles, identified by literature search. Additionally, heatmap data for miRs showing a strong correlation (correlation ≥±0.5) with either troponin AUC or edema, infarct size or salvage index (measured by MRI) are shown in the table. Where a miR is found in one or more principal components, the component numbers are shown. Tissue origin information is from Tissue Atlas [34] (https://ccb-web.cs.uni-saarland.de/tissueatlas/patterns) unless otherwise cited.

In addition to these relationships between miRs and myocardial injury, we also observed that other non-myomiRs, which have been associated with biological processes such as endothelial cell injury, inflammation and platelet activation were strongly associated with either early myocardial injury or late outcome, including miRs-126-3p, 152-3p, 181a-2-3p and 200a-3p. The putative biological functions and associations of these miRs are shown in Table 2.

Transcoronary miR release

In order to evaluate the specific contribution of acute cardiac injury to the levels of circulating miRs, we quantified the trans-myocardial gradient of miR concentrations from blood samples drawn from the coronary artery and the coronary sinus, after coronary stent placement but before completing the PPCI procedure. Concentrations of known myomiRs increased between coronary artery and coronary sinus (e.g. miR-133a, -499a) (Fig. 3), or were undetectable in the coronary artery and became detectible in the coronary sinus (e.g. miR-1, -208a). Other miRs not previously associated with myocardial infarction also increased down the coronary gradient and showed a strong correlation with troponin release (e.g. miR-99a, -125b, -145, -378a). A subset of miRs decreased between coronary artery and coronary sinus, such as miR-337, -28 and -671, or was detectible in the coronary artery samples but not the coronary sinus samples (e.g. miR-204, -256) (Supplementary data figure 6, Supplemental digital content 1, *http://links.lww.com/MCA/A599*).

miR release by endothelial cells

We next sought to identify miRs that are released in acute STEMI and associated with endothelial cell injury, using an in vitro model of human endothelial cells exposed to hypoxia. Fewer miRs were detected in endothelial cell culture supernatant compared with human plasma samples (median 174 and 253 respectively, $P \leq 0.001$). In particular, none of the previously described plasma myomiRs were detected in endothelial cell supernatants. Exposure of endothelial cells to hypoxia led to an increase in a subset of miRs (e.g. let-7g, miR-1271) whereas some miRs decreased in response to hypoxia (e.g. let-7d, miR-1245a) (Supplementary data figure 7, Supplemental digital content 1, *http://links.lww.com/MCA/A599*). These data indicate that acute endothelial cell injury is an important component of the response to acute STEMI, and can be detected by quantification of miRs in peripheral blood samples.

Developing an integrated biomarker model to predict outcome after STEMI

In order to combine the predictive value of the miRs identified in the unbiased screen, we developed regression models to estimate the extent of acute myocardial injury (area at risk), final infarct size and salvage index,

Fig. 3

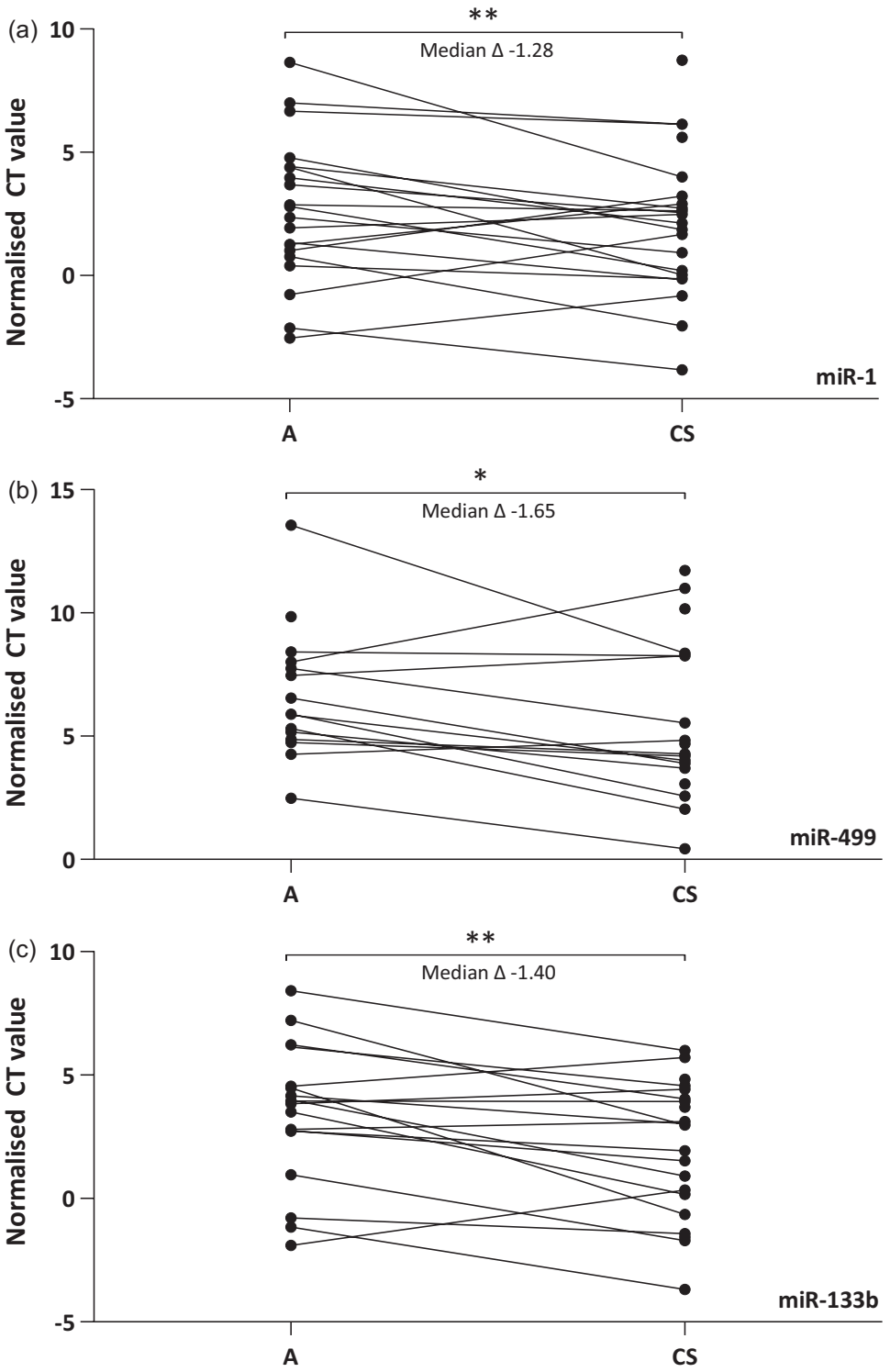

Changes in miR concentration between coronary artery (a) and coronary sinus (CS). Samples were paired (artery and vein samples were collected from patients patient during a single procedure). (a) miR-1 (median change in normalized CT value −1.28); (b) miR-499 (median change -1.65); (c) miR-133-b (median change −1.40).

Fig. 4

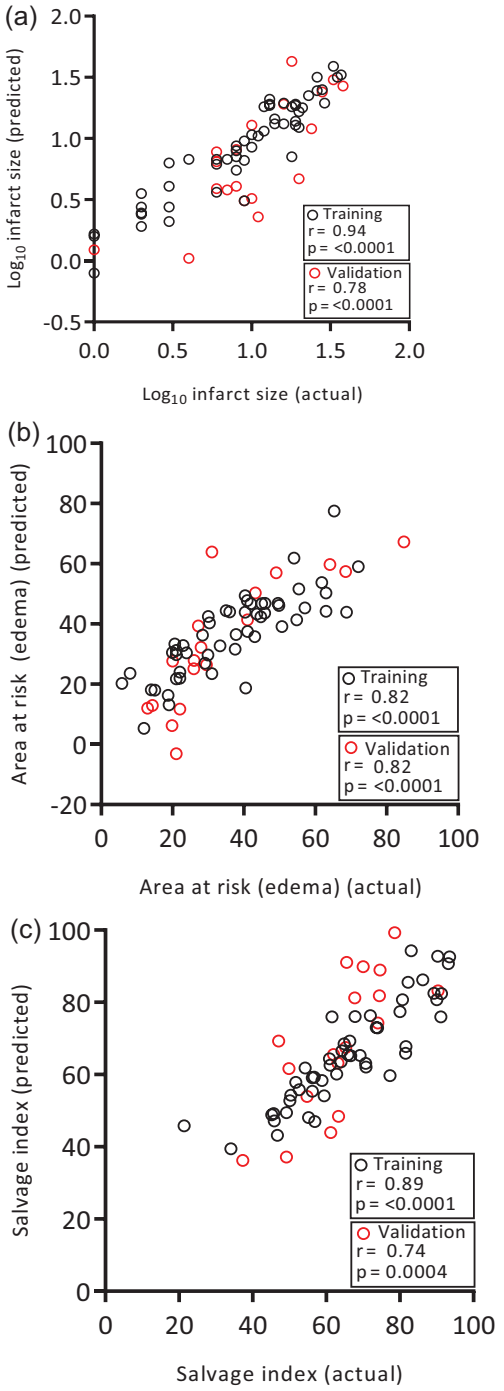

Predictive models for infarct size, myocardial edema and salvage index Multiple regression models to predict infarct size (panel a), myocardial edema (b) and salvage index (c) were designed using troponin and multiple miRs (Table 2), all measured 6 hours after primary PCI. The model was designed using a randomly allocated training cohort of 80% of patients and then validated with the remaining 20% of patients.

each determined by cardiac MRI, using a selected number of miRs quantified in a single blood sample 6 hours after PPCI.

For the infarct size prediction model, miRs 145-5p, 151a-3p, 18a-3p, 219a-5p, 424-3p, 941, 99a-5p, let-7d-5p, let-7e-5p and troponin at 6 hours were selected as variables using forward stepwise model selection to identify a group of strongly predictive miRs. The previously reported clinical associations of these miRs are shown in Table 2. A multiple linear regression model was developed using the training cohort and, using this model, the predicted infarct size strongly correlated with actual infarct size (r = 0.94, $P \leq 0.0001$). This model was then validated using the separate validation cohort, yielding a similarly strong correlation between predicted and actual infarct size (r = 0.78, $P \leq 0.0001$) (Fig. 4).

Using the same techniques, predictive models for myocardial edema (area at risk) and salvage index were created. For the myocardial edema (area at risk) model, miRs 145-3p, 200a-3p, 23b-3p, 362-5p, 7-1-3p, let-7a-5p, let-7c-3p and troponin at 6 hours were identified as variables. The correlation between predicted and actual edema was 0.82 ($P \leq 0.0001$) and 0.82 ($P = 0.001$) in the training and validation cohorts, respectively. For the salvage index model, miRs 154-5p, 299-5p, 381-3p, 423-3p, 424-3p, 501-3p, 7-1-3p, 887-3p and troponin at 6 hours were identified as the predictive variables. The correlation between the predicted and actual salvage index was 0.89 ($P \leq 0.0001$) and 0.74 ($P \leq 0.0001$) in the training and validation cohorts, respectively (Fig. 4).

Discussion

This study reveals new insights into the importance of miR release after STEMI as biomarkers of the myocardial and systemic response to acute MI, with major implications for understanding both pathophysiologic mechanisms in STEMI and in predicting early and late clinical outcomes.

First, this study provides the first systematic and comprehensive profiling of circulating miRs immediately after STEMI, identifying a number of miRs not previously recognized to be associated with the myocardial and systemic responses to MI. These newly implicated miRs are likely to have biological roles in regulating key aspects of STEMI pathogeneses, including vascular injury, endothelial dysfunction, inflammation and platelet activation. Accordingly, the comprehensive quantification of miR release after STEMI identifies new pathways that may be targeted for therapeutic intervention. Second, systematic profiling of miRs after STEMI, rather than only selected miRs known to be associated with myocardial necrosis, provides circulating biomarkers that are associated with clinically important outcomes. Specifically, we demonstrate that quantification of a small group of selected miRs can provide a powerful predictor of acute area at risk, final infarct size and salvage index, all derived from a single blood sample taken 6 hours after primary PCI. Taken together, these

findings have important implications for new biological understanding of pathophysiologic mechanisms in STEMI, for patient stratification, selection and risk prediction, and for quantification of outcomes after STEMI. Since these insights are based on a single sample at an early time point after STEMI, there are direct clinical implications for early patient stratification and treatment, rather than waiting for the subsequent evolution of post-STEMI pathophysiology, by which time opportunities for intervention or therapy may have been missed.

We achieved high analytic power through the Oxford Acute Myocardial Infarction (OxAMI) study, with its a well-established systematic data and blood sample collection, in the emergency setting of primary PCI [23–25]. Patients with pain onset of greater than 12 h were excluded, as were patients with greater than TIMI 0/1 flow, which minimized the risk of confounding by any late-presenting MI, spontaneous reperfusion or non-STEMI. By co-locating the blood sample processing laboratory adjacent to the cardiac catheter lab, blood samples could be processed and frozen rapidly, minimizing risk of sample degradation, or inconsistency. We used a rigorous protocol for generation of platelet-poor plasma, since residual platelet contamination can confound miR analysis, with a robust miR processing quality control algorithm, including controls for sample hemolysis and RT-PCR efficiency, ensuring that any technically inadequate samples or results were identified and either verified or discarded [26].

The total number of human miRs detectable in plasma after STEMI has not previously been reported. By undertaking an unbiased analysis of all detectable miRs, at four time points (0, 6, 24 and 48 h), we found that more than 200 miRs were detectable, with a greater number detected at the 6, 24 and 48-hour time points than after the 0-hour time point, likely reflecting the increase in the levels and number of circulating miRs after STEMI. From the unbiased 'discovery' experiment we undertook serial triage to select analytical sets of 384 and then 128 miRs and controls, thereby allowing the greater sample throughput necessary to undertake miR analysis in a larger number of patients, enabling associations between miRs and clinical outcomes.

Within this comprehensive dataset, we found that the known myocardial miRs, previously shown to be elevated in acute myocardial infarction, when measured 6 hours after PCI, have a strong correlation with final infarct size measured by MRI at 6 months. The strength of this relationship is perhaps surprising, given the temporal difference between the two tests (6 h after PCI vs. 6 months after PCI), although a similar relationship was seen with plasma troponin level. However, we found that several other miRs correlated with troponin and infarct size, relationships that have not previously been reported. By measuring paired coronary artery and coronary sinus samples, we were able to show for the first time that known myomiRs (e.g. miR-1, -499, -208a) either increased in concentration or became measurable down the transcoronary gradient, strongly suggesting dynamic myocardial release. Other miRs not previously shown to be associated with myocardial injury showed similar patterns of release (e.g. miR-99a, -125b, -145, -378a, -337, -28, -671, -204, -256).

We also observed, in human STEMI, important new associations with miRs implicated in biological processes. For example, miR 126-3p has received substantial attention as a marker of endothelial injury, platelet activation and angiogenesis. Our observation that miR126 release after STEMI correlates with acute myocardial injury and late infarct size highlights the potential importance of coronary microvascular injury as a pathophysiologic mechanism in STEMI, and a potential therapeutic target. Indeed, miR126 expression by endothelial progenitor cells reduced infarct size in an experimental MI model [27]. Other novel miRs associated with the response to STEMI included, miR-181a-2-3p, miR-200a-3p and miR-25-3p. miR-181a-2-3p plays a role in stem cell growth or apoptosis via the EGF/PI3K/SOX2 axis [28]. miR-200a-3p has been identified as a biomarker in cancers, and alters SIRT-1 signaling [29,30]. Exosomal miR-25-3p mediates signals from cancer cells to endothelial cells, targeting KLF2 and KLF4, that stimulate vascular permeability and angiogenesis, raising the possibility of similar roles in the response to coronary microvascular injury after STEMI [31,32].

It has previously been shown that miR expression is highly tissue-specific [33]. Our quantification of miR release showed that none of the myomiRs (either previously reported or identified in this study) were released from in vitro endothelial cells. In addition, fewer miRs are detected in these cells than in human plasma. The effect on miR release of a hypoxic insult on endothelial cells has not previously been reported. The luminescent assay confirmed that hypoxia was having the expected deleterious effect on cell viability. In a subset of miRs, there was a dose dependent response to hypoxia, such as let-7g, miR-1271 (increased with hypoxia) and let-7d and miR-1245a (decreased).

Whilst myocardial injury and final infarct size were strongly correlated with selected individual miRs, we used PCA to identify the miR signatures of myocardial infarction using an unbiased statistical approach. This method decomposes and ranks the major axes of variation in the data. Principal component 1, the strongest axis of variation, correlated with markers of myocardial necrosis (troponin release, infarct size, salvage index). Component 2 correlated with markers of recovery (ST-segment resolution after PCI, left ventricular ejection fraction at 6 months). Other components correlated with clinical

parameters such as hemoglobin, cholesterol, renal function and blood gas measurements. These associations between novel miR signatures and clinical outcomes after STEMI will provide new opportunities for understanding the pathobiology of acute myocardial infarction.

Rapid and accurate diagnostic tests are needed for clinical assessment after myocardial infarction, to ensure that patients receive the appropriate management, to stratify those patients requiring more intensive treatment strategies, to measure the success or otherwise of primary PCI, and to effectively identify patients suitable for research studies or targeted clinical trials. These parameters are typically quantified using cardiac MRI which is time-consuming, expensive, and may be difficult for a patient to tolerate soon after myocardial infarction. Moreover, infarct size and salvage index are currently measured months after myocardial infarction, whereas it would be useful to have earlier indicators of clinical outcome.

Since we systematically characterized the miR profile after STEMI, we used our findings to design models to predict myocardial injury, infarct size and salvage index, by quantifying selected miRs in a single blood test taken 6 hours after PPCI. Using a panel of nine miRs, combined with plasma troponin, the infarct size model was able to predict final infarct size (measured by MRI at 6 months) with high accuracy. This finding has important clinical implications. For example, risk of ventricular arrhythmia strongly correlates with infarct size and identifying patients at high risk could ensure proactive diagnosis and treatment (e.g. more intensive monitoring, up-titration of beta blockers and earlier referral for device therapy), whereas patients with a low miR-based prediction of infarct size could be rehabilitated more rapidly.

The 'area at risk' (AAR), quantified by myocardial edema measured by cardiac MRI in the first 48 h after STEMI, is an indication of the maximal extent of myocardial ischemia-reperfusion injury subtended by the occluded infarct-related artery. Combined with final infarct size, AAR allows calculation of the salvage index (AAR - final infarct size/ area at risk) which measures the success or otherwise of reperfusion therapy. Calculation of these indices requires at least two cardiac MRI scans, one done at >3 months after STEMI. Furthermore, the optimal timing of cardiac MRI to quantify AAR in humans remains uncertain [34]. We were able to predict both AAR (myocardial edema) and salvage index using a panel of 9 miRs quantified in a single blood test taken 6 hours after PPCI. Prediction of myocardial edema, infarct size and salvage index from a single blood sample, without recourse to serial cardiac MRI, and overcoming the clinical and logistic challenges of such studies in STEMI patients, has the potential to enhance and accelerate patient stratification and management early after PPCI, and may provide new more convenient and cost-effective end points in clinical trials.

Conclusion

We used an unbiased approach to systematically quantify all known human miRs in plasma, at time points after PPCI for STEMI. We found both known and novel miRs correlated with myocardial injury, but by PCA we identified groups of miRs that were strongly associated with important clinical outcomes, and implicated biological processes such as microvascular injury, platelet activation and inflammation in the pathophysiological response to STEMI. From a single blood sample taken 6 hours after PPCI, we derived predictive models based on a small sub-group of miRs, that are able to predict both early myocardial injury (area at risk), late myocardial damage (final infarct size) and myocardial salvage index. These new findings have the potential to reveal novel biological aspects in the local and systemic response to myocardial infarction and provide a rapid and convenient early predictive model for patient stratification and management early after STEMI, without the need for repeated imaging over the months following STEMI.

Acknowledgements

The authors would like to thank the OxAMI research nurses and all the members of the Oxford Catheterization Laboratory and Coronary Care Unit for their support of this work. We would also like to thank the Bioinformatics CRO, Inc. for their input with statistical analysis.

This work was supported by the Oxford British Heart Foundation (BHF) Centre of Research Excellence (RG/13/1/30181), BHF Chair Award (CH/16/1/32013), and the National Institute for Health (NIHR) Oxford Biomedical Research Centre.

Conflicts of interest

There are no conflicts of interest.

References

1 British Heart Foundation. Cardiovascular disease statistics. https://www.bhf.org.uk/what-we-do/our-research/heart-statistics. [Accessed 1 September 2023].
2 Weaver WD, Simes RJ, Betriu A, Grines CL, Zijlstra F, Garcia E, *et al*. Comparison of primary coronary angioplasty and intravenous thrombolytic therapy for acute myocardial infarction: a quantitative review. *JAMA* 1997; **278**:2093–2098.
3 Growth of Primary PCI for the treatment of heart attack patients in England 2008-2011: the role of NHS Improvement and the Cardiac Networks. *NHS Improv* 2012.
4 Cuculi F, Caterina ARD, Kharbanda RK, Banning AP. Optimal reperfusion in ST-elevation myocardial infarction--the role of the coronary microcirculation. *Swiss Med Wkly* 2011; **141**:2–10.
5 Wu KC, Kim RJ, Bluemke DA, Rochitte CE, Zerhouni EA, Becker LC, *et al*. Quantification and time course of microvascular obstruction by contrast-enhanced echocardiography and magnetic resonance imaging following acute myocardial infarction and reperfusion. *J Am Coll Cardiol* 1998; **32**:1756–1764.
6 Klug G, Mayr A, Schenk S, Esterhammer R, Schocke M, Nocker M, *et al*. Prognostic value at 5 years of microvascular obstruction after acute

myocardial infarction assessed by cardiovascular magnetic resonance. *J Cardiovasc Magn Reson* 2012; **14**:46.

7 Tzivoni D, Koukoui D, Guetta V, Novack L, Cowing G; CASTEMI Study Investigators. Comparison of troponin t to creatine kinase and to radionuclide cardiac imaging infarct size in patients with ST-elevation myocardial infarction undergoing primary angioplasty. *Am J Cardiol* 2008; **101**:753–757.

8 Dall'Armellina E, Karia N, Lindsay AC, Karamitsos TD, Ferreira V, Robson MD, *et al*. Dynamic changes of edema and late gadolinium enhancement after acute myocardial infarction and their relationship to functional recovery and salvage index. *Circ Cardiovasc Imaging* 2011; **4**:228–236.

9 Ruparelia N, Chai JT, Fisher EA, Choudhury RP, Hospital JR, Way H, *et al*. Inflammatory processes in cardiovascular disease: a route to targeted therapies. *Nat Rev Cardiol* 2017; **14**:133–144.

10 Bartel DP, Lee R, Feinbaum R. MicroRNAs. Genomics, biogenesis, mechanism, and function genomics: the miRNA genes. *Cell* 2004; **116**:281–297.

11 Mitchell PS, Parkin RK, Kroh EM, Fritz BR, Wyman SK, Pogosova-Agadjanyan EL, *et al*. Circulating microRNAs as stable blood-based markers for cancer detection. *Proc Natl Acad Sci U S A* 2008; **105**:10513–10518.

12 Cheng C, Wang Q, You W, Chen M, Xia J. MiRNAs as biomarkers of myocardial infarction: a meta-analysis. *PLoS One* 2014; **9**:e88566.

13 Meder B, Keller A, Vogel B, Haas J, Sedaghat-Hamedani F, Kayvanpour E, *et al*. MicroRNA signatures in total peripheral blood as novel biomarkers for acute myocardial infarction. *Basic Res Cardiol* 2011; **106**:13–23.

14 Lalem T, Devaux Y. Circulating microRNAs to predict heart failure after acute myocardial infarction in women. *Clin Biochem* 2019; **70**:1–7.

15 Sahan KM, Channon KM, Choudhury RP, Kharbanda RK, Lee R, Sheehan M. Refining the enrolment process in emergency medicine research. *Eur. J. Cardiovasc. Med* 2016; **4**:506–510.

16 Lee R, Antonopoulos AS, Alexopoulou Z, Margaritis M, Kharbanda RK, Choudhury RP, *et al*. Artifactual elevation of plasma sCD40L by residual platelets in patients with coronary artery disease. *Int J Cardiol* 2013; **168**:1648–1650.

17 Cuculi F, Dall'Armellina E, Manlhiot C, Caterina ARD, Colyer S, Ferreira V, *et al*. Early change in invasive measures of microvascular function can predict myocardial recovery following PCI for ST-elevation myocardial infarction. *Eur Heart J* 2014; **35**:1971–1980.

18 Patel N, Petraco R, Dall'Armellina E, Kassimis G, Maria GLD, Dawkins S, *et al*. Zero-flow pressure measured immediately after primary percutaneous coronary intervention for st-segment elevation myocardial infarction provides the best invasive index for predicting the extent of myocardial infarction at 6 months: An OxAMI study (Oxford Acute Myocardial Infarction). *JACC Cardiovasc Interv* 2015; **8**:1410–1421.

19 Andersen CL, Jensen JL, Ørntoft TF. Normalization of real-time quantitative reverse transcription-PCR data: a model-based variance estimation approach to identify genes suited for normalization, applied to bladder and colon cancer data sets. *Cancer Res* 2004; **64**:5245–5250.

20 Yang Y, Xu Z, Song D. Missing value imputation for microRNA expression data by using a GO-based similarity measure. *BMC Bioinf* 2015; **17**(Suppl 1):10:109–116.

21 Yang H. The case for being automatic: introducing the automatic linear modeling (LINEAR) procedure in SPSS statistics. *Mult Linear Regres Viewpoints* 2013; **39**:27–37.

22 Eitel I, Adams V, Dieterich P, Fuernau G, de Waha S, Desch S, *et al*. Relation of circulating MicroRNA-133a concentrations with myocardial damage and clinical prognosis in ST-elevation myocardial infarction. *Am Heart J* 2012; **164**:706–714.

23 Ruparelia N, Godec J, Lee R, Chai JT, Dall'Armellina E, McAndrew D, *et al*. Acute myocardial infarction activates distinct inflammation and proliferation pathways in circulating monocytes, prior to recruitment, and identified through conserved transcriptional responses in mice and humans. *Eur Heart J* 2015; **36**:1923–1934.

24 Maria GLD, Fahrni G, Alkhalil M, Cuculi F, Dawkins S, Wolfrum M, *et al*. A tool for predicting the outcome of reperfusion in ST-elevation myocardial infarction using age, thrombotic burden and index of microcirculatory resistance (ATI score). *EuroIntervention* 2016; **12**:1223–1230.

25 Patel N, Petraco R, Dall'Armellina E, Kassimis G, Maria GLD, Dawkins S, *et al*. Zero-flow pressure measured immediately after primary percutaneous coronary intervention for ST-segment elevation myocardial infarction provides the best invasive index for predicting the extent of myocardial infarction at 6 months: an OxAMI study (Oxford. *JACC Cardiovasc Interv* 2015; **8**:1410–1421.

26 Mitchell AJ, Gray WD, Hayek SS, Ko YA, Thomas S, Rooney K, *et al*. Platelets confound the measurement of extracellular miRNA in archived plasma. *Sci Rep* 2016; **6**:1–11.

27 Li H, Liu Q, Wang N, Xu Y, Kang L, Ren Y, *et al*. Transplantation of endothelial progenitor cells overexpressing miR-126-3p improves heart function in ischemic cardiomyopathy. *Circ J* 2018; **82**:2332–2341.

28 Lakomy R, Sana J, Hankeova S, Fadrus P, Kren L, Lzicarova E, *et al*. MiR-195, miR-196b, miR-181c, miR-21 expression levels and O-6-methylguanine-DNA methyltransferase methylation status are associated with clinical outcome in glioblastoma patients. *Cancer Sci* 2011; **102**:2186–2190.

29 Landgraf P, Rusu M, Sheridan R, Sewer A, Iovino N, Aravin A, *et al*. A mammalian microRNA expression atlas based on small RNA library sequencing. *Cell* 2007; **129**:1401–1414.

30 Li X, Roslan S, Johnstone CN, Wright JA, Bracken CP, Anderson M, *et al*. MiR-200 can repress breast cancer metastasis through ZEB1-independent but moesin-dependent pathways. *Oncogene* 2014; **33**:4077–4088.

31 Chen H, Pan H, Qian Y, Zhou W, Liu X. MiR-25-3p promotes the proliferation of triple negative breast cancer by targeting BTG2. *Mol Cancer* 2018; **17**:1–11.

32 Zeng Z, Li Y, Pan Y, Lan X, Song F, Sun J, *et al*. Cancer-derived exosomal miR-25-3p promotes pre-metastatic niche formation by inducing vascular permeability and angiogenesis. *Nat Commun* 2018; **9**:5395.

33 Mccall MN, Kent OA, Yu J, Fox-talbot K, Zaiman AL, Halushka MK. MicroRNA profiling of diverse endothelial cell types. *BMC Med Genomics* 2011; **4**:78.

34 Fernández-Jiménez R, Barreiro-Pérez M, Martin-García A, Sánchez-González J, Agüero J, Galán-Arriola C, *et al*. Dynamic edematous response of the human heart to myocardial infarction. *Circulation* 2017; **136**:1288–1300.

35 Ludwig N, Leidinger P, Becker K, Backes C, Fehlmann T, Pallasch C, *et al*. Distribution of miRNA expression across human tissues. *Nucleic Acids Res* 2016; **44**:3865–3877.

36 Langley RR, Ramirez KM, Tsan RZ, Van Arsdall M, Nilsson MB, Fidler IJ. Tissue-specific microvascular endothelial cell lines from H-2K(b)-tsA58 mice for studies of angiogenesis and metastasis. *Cancer Res* 2003; **63**:2971–2976.

37 Tsang WP, Kwok TT. The miR-18a* microRNA functions as a potential tumor suppressor by targeting on K-Ras. *Carcinogenesis* 2009; **30**:953–959.

38 Majid S, Dar AA, Saini S, Deng G, Chang I, Greene K, *et al*. MicroRNA-23b Functions as a tumor suppressor by regulating Zeb1 in bladder cancer. *PLoS One* 2013; **8**:e67686.

39 Lin KY, Ye H, Han BW, Wang WT, Wei PP, He B, *et al*. Genome-wide screen identified let-7c/miR-99a/miR-125b regulating tumor progression and stem-like properties in cholangiocarcinoma. *Oncogene* 2016; **35**:3376–3386.

40 Cui SY, Wang R, Chen LB. MicroRNA-145: a potent tumour suppressor that regulates multiple cellular pathways. *J Cell Mol Med* 2014; **18**:1913–1926.

41 Lin C, Li Z, Chen P, Quan J, Pan X, Zhao L, *et al*. Oncogene miR-154-5p regulates cellular function and acts as a molecular marker with poor prognosis in renal cell carcinoma. *Life Sci* 2018; **209**:481–489.

42 Zhuang C, Yuan Y, Song T, Wang H, Huang L, Luo X, *et al*. miR-219a-5p inhibits breast cancer cell migration and epithelial-mesenchymal transition by targeting myocardin-related transcription factor a. *Acta Biochim Biophys Sin (Shanghai)* 2017; **49**:1112–1121.

43 Wu K, Yang L, Chen J, Zhao H, Wang J, Xu S, *et al*. miR-362-5p inhibits proliferation and migration of neuroblastoma cells by targeting phosphatidylinositol 3-kinase-C2β. *FEBS Lett* 2015; **589**:1911–1919.

44 Xu Y, Ohms SJ, Li Z, Wang Q, Gong G, Hu Y, *et al*. Changes in the expression of miR-381 and miR-495 are inversely associated with the expression of the MDR1 gene and development of multi-drug resistance. *PLoS One* 2013; **8**:e82062–e82013.

45 Zhang J, Du Y, Wu C, Ren X, Ti X, Shi J, *et al*. Curcumin promotes apoptosis in human lung adenocarcinoma cells through miR-186* signaling pathway. *Oncol Rep* 2010; **24**:1217–1223.

46 Rodriguez-Barrueco R, Nekritz EA, Bertucci F, Yu J, Sanchez-Garcia F, Zeleke TZ, *et al*. miR-424(322)/503 is a breast cancer tumor suppressor whose loss promotes resistance to chemotherapy. *Genes Dev* 2017; **31**:553–566.

47 Chow TF, Mankaruos M, Scorilas A, Youssef Y, Girgis A, Mossad S, *et al*. The miR-17-92 cluster is over expressed in and has an oncogenic effect on renal cell carcinoma. *J Urol* 2010; **183**:743–751.

48 Fite K, Gomez-Cambronero J. Down-regulation of MicroRNAs (MiRs) 203, 887, 3619 and 182 prevents vimentin-triggered, phospholipase D (PLD)-mediated cancer cell invasion. *J Biol Chem* 2016; **291**:719–730.
49 Hu HY, He L, Fominykh K, Yan Z, Guo S, Zhang X, *et al*. Evolution of the human-specific microRNA miR-941. *Nat Commun* 2012; **3**:1110–1145.
50 Rijavec M, Korošec P, Žavbi M, Kern I, Malovrh MM. Let-7a is differentially expressed in bronchial biopsies of patients with severe asthma. *Sci Rep* 2014; **4**:1–5.
51 Zhou Z, Lu X, Wang J, Xiao J, Liu J, Xing F. MicroRNA let-7c is essential for the anisomycin-elicited apoptosis in Jurkat T cells by linking JNK1/2 to AP-1/STAT1/STAT3 signaling. *Sci Rep* 2016; **6**:1–13.
52 Kolenda T, Przybyla W, Teresiak A, Mackiewicz A, Lamperska KM. The mystery of let-7d - a small RNA with great power. *Contemp Oncol (Pozn)* 2014; **18**:293–301.
53 Lin Z, Ge J, Wang Z, Ren J, Wang X, Xiong H, *et al*. Let-7e modulates the inflammatory response in vascular endothelial cells through ceRNA crosstalk. *Sci Rep* 2017; **7**:1–12.